KINEMATICS AND SINGULARITY ANALYSIS OF A CRRHHRRC PARALLEL SCHÖNFLIES MOTION GENERATOR

Takashi Harada[1] and Jorge Angeles[2]
[1]*Department of Mechanical Engineering, Faculty of Science and Engineering, Kinki University, Higashiosaka, Osaka, Japan*
[2]*Department of Mechanical Engineering and Center for Intelligent Machines, McGill University, Montreal, Quebec, Canada*
E-mail: harada@mech.kindai.ac.jp; angeles@cim.mcgill.ca

Received July 2013, Accepted March 2014
No. 13-CSME-141, E.I.C. Accession 3599

ABSTRACT
A novel architecture for a parallel Schönflies motion generator was recently proposed, consisting of a CRRHHRRC linkage. The novelty of this architecture lies in its simplicity, as it comprises only two limbs, thereby forming a single-loop closed kinematic chain. Reported in this paper is a realization of this architecture, intended for the production of a proof-of-concept prototype. The realization includes an innovative actuator mechanism, which is based on two-degree-of-freedom cylindrical joints. Moreover, its moving plate is coupled to the two limbs by means of corresponding coaxial H pairs. The paper focuses on the kinematics and singularity analysis of this robot, intended for fast pick-and-place operations. The prototype is currently under development at McGill University's Centre for Intelligent Machines.

Keywords: Schönflies motion generators; kinematics; Jacobian analysis; singularity analysis.

ANALYSES CINÉMATIQUE ET DE SINGULARITÉ D'UN ROBOT PARALLÈLE CRRHHRRC POUR LA PRODUCTION DE MOUVEMENTS DE SCHÖNFLIES

RÉSUMÉ
Une nouvelle architecture de robot parallèle de type CRRHHRRC destinée à la production de mouvements de Schönflies a récemment faite son apparition dans la littérature. Cette architecture est novatrice en ce sens qu'elle est simple, car elle ne comporte que deux bras, ce qui donne une chaîne cinématique à une seule boucle. Les auteurs proposent ici une réalisation de cette architecture, destinée à un prototype expérimental, qui comporte un mécanisme d'actuation basé sur des articulations cylindriques à deux degrés de liberté. En outre, les deux bras sont couplés à la plate-forme mobile par des articulations cinématiques coaxiales de type H. Cette communication fait le point sur la cinématique et l'analyse de singularité de ce robot, qui est destiné aux opérations de transfert rapide, dont un prototype fait l'objet de travaux au Centre de recherche sur les machines intelligentes de l'Université McGill.

Mots-clés : Mécanismes pour la production de mouvements de Schönflies ; cinématique ; analyse de la jacobienne ; analyse de singularité.

1. INTRODUCTION

Schönflies motions comprise three translations and one rotation, as occurring on the motions of a waiter's tray, occur frequently in pick-and-place operations. Robots for industrial assembly and packaging, capable of these motions are thus termed Schönflies motion generators (SMGs). Current R&D work in connection with SMGs targets fast operations, their performance being measured by the number of test cycles that can be executed by these robots in one second. The record is three cycles per second on an industry-adopted trajectory: 25 mm up from a moving-plate (MP) home pose, followed by a 300 mm horizontal path, down 25 mm and back to the home pose following the same path in the opposite direction. Moreover, during the horizontal segment of the path, the MP is to turn 180° cw in the first half of the cycle, 180° ccw when returning.

Some parallel robots producing Schönflies motion can be cited: The McGill SMG [1], the H4 [2, 3], I4L, I4R, Heli and Par4. Adept Technology's Quattro is the fastest SMG in the market. Quattro is supplied with four limbs that connect the MP with the base plate (BP). In the Quattro and I4L, the rotation is obtained through gear trains, to provide for a rotation amplification [3]. The latter is needed because of the low rotatability of the MP by virtue of the four limbs, which contributes to the overall complexity of the robot. Recently, an alternative architecture was proposed by Lee and Lee [4], which entails coaxial helical (H) joints[1] to achieve the rotation of the MP. H pairs being available off-the-shelf, a coaxial HH subchain can be readily designed for producing a full rotation of the MP. Research on the feasibility of a HH mechanism, along with the kinematics, dynamics, optimum design, prototyping, and control of a SMG with Lee and Lee's architecture, dubbed the *Peppermill* because of the resemblance of its MP with a large wooden peppermill, is now underway at McGill University's *Centre for Intelligent Machines*, in collaboration with Japan's Kinki University. In this paper, the kinematic model, position and velocity analysis of the HH mechanism are introduced as a first step of the feasibility study. The singularities of the mechanism are identified.

2. KINEMATIC MODEL OF THE PEPPERMILL

A schematic view of the Peppermill is illustrated in Fig. 1. Two CRR limbs are connected to the MP, that carries a coaxial subchain of H joints. The Peppermill is made up of a single-loop linkage of the CRRHHRRC type. The C joints of the linkage are driven by identical rotational motors in a differential array of ball-screw drives (see Appendix A); the axis of the ith C joint, for $i = 1, 2$, termed here the ith-drive axis, is parallel to the fixed unit vector $\mathbf{a}_i$. Moreover, d_i and θ_i denote the translational and rotational displacement variables of the ith limb, respectively, with d_i measured in units of length, θ_i in radians. That is, d_i and θ_i are the *actuator variables*. Points O_i denote the intersection of the ith-drive axis with the common normal to the two, which is the z-axis of the base frame.

The fixed origin O of the base frame is set at the midpoint of segment $\overline{O_1O_2}$, as shown in Fig. 1. Unit vectors parallel to the x, y and z axes are defined as $\mathbf{i}$, $\mathbf{j}$ and $\mathbf{k}$, respectively. The angle of rotation of the proximal passive R joint is defined as λ_i, while $\mathbf{u}_i$ and $\mathbf{v}_i$ are unit vectors parallel to the axes of the proximal and the distal links of the ith limb, respectively. Furthermore, r_i and l_i denote the lengths of these links. The end of the distal link of the ith limb is coupled with the passive R pair of the MP at point P_i. The pose of the MP is given by $\mathbf{c} = [x, y, z]^T$, the position vector of point C, and angle ϕ, as shown in Fig. 1. Angle ϕ, in turn, is measured from a predefined orientation of the axially symmetric MP.

[1] In this paper, the standard nomenclature of kinematic chains is used, whereby C, H and R denote, respectively, cylindrical, helical (or screw) and revolute kinematic pairs.

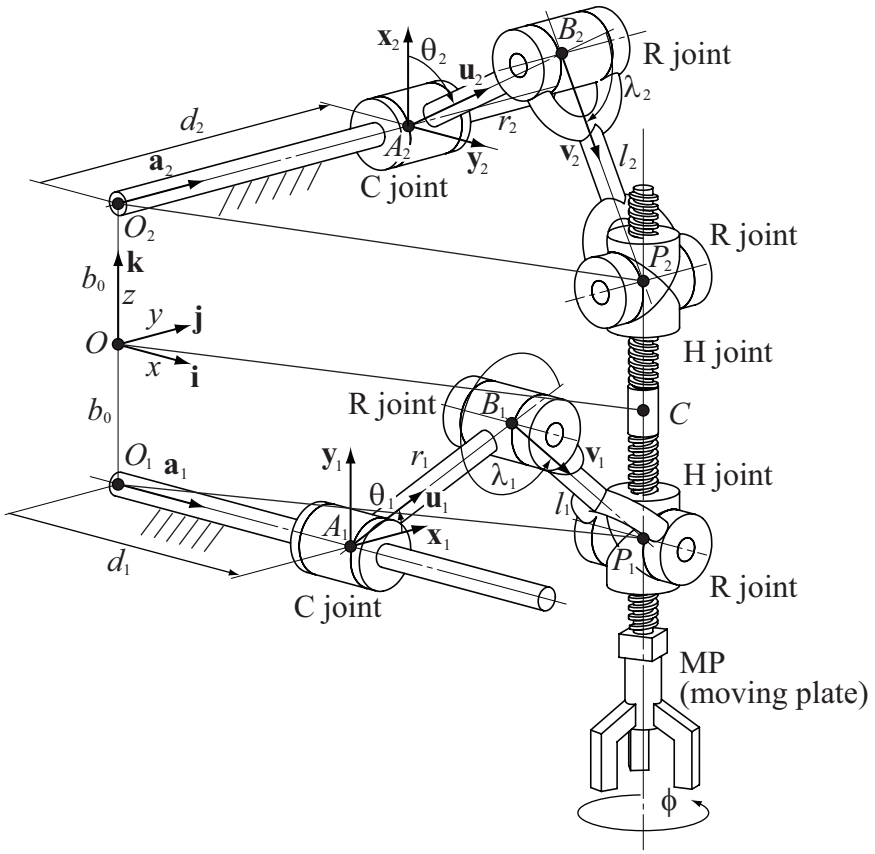

Fig. 1. Schematic view of CRRHHRRC Parallel SMG (the Peppermill).

3. DISPLACEMENT ANALYSIS OF THE PEPPERMILL

3.1. Vector Loop Equations

Vector $\overrightarrow{O_iP_i}$ is described upon following two paths[2]:

$$\mathbf{p}_i = \overrightarrow{O_iP_i} = \overrightarrow{O_iA_i} + \overrightarrow{A_iB_i} + \overrightarrow{B_iP_i} \tag{1}$$

$$\mathbf{p}_i = \overrightarrow{O_iP_i} = \overrightarrow{O_iO} + \overrightarrow{OC} + \overrightarrow{CP_i} \tag{2}$$

The first expression is obtained along the ith limb, the second via point C of the MP; the two paths are shown in Fig. 1. Therefore, the first expression involves actuator coordinates d_i and θ_i, the second the Cartesian coordinates of the MP, namely, x, y, z and ϕ.

The various vectors appearing in the rightmost-hand side of Eq. (1) are readily expressed in terms of actuator variables, namely,

$$\overrightarrow{O_iA_i} = d_i\mathbf{a}_i, \quad \overrightarrow{O_1A_1} = d_1\mathbf{i}, \quad \overrightarrow{O_1A_1} = d_2\mathbf{j} \tag{3}$$

Moreover,

$$\overrightarrow{A_iB_i} = r_i\mathbf{u}_i(\theta_i) \tag{4}$$

[2]Henceforth, every time a relation involving subscript i will be understood to apply to $i = 1, 2$.

where

$$\mathbf{u}_i(\theta_i) = \cos\theta_i \mathbf{x}_i + \sin\theta_i \mathbf{y}_i \tag{5}$$

In Eq. (5), $\mathbf{x}_i$ and $\mathbf{y}_i$ denote unit vectors of the coordinates frame at A_i as shown in Fig. 1. Moreover,

$$\overrightarrow{B_iP_i} = l_i \mathbf{v}_i(\theta_i, \lambda_i) \tag{6}$$

with

$$\mathbf{v}_i(\theta_i, \lambda_i) = \cos(\theta_i + \lambda_i)\mathbf{x}_i + \sin(\theta_i + \lambda_i)\mathbf{y}_i \tag{7}$$

Expressions for vectors in the rightmost-hand side of Eq. (2) are given below:

$$\overrightarrow{O_iO} = -\overrightarrow{OO_i}, \quad \overrightarrow{OO_i} = \mathbf{o}_i = b_{0i}\mathbf{k} \tag{8}$$

$$\overrightarrow{OO_1} = \mathbf{o}_1 = -b_0\mathbf{k}, \quad \overrightarrow{OO_2} = \mathbf{o}_2 = b_0\mathbf{k} \tag{9}$$

In the second of Eqs. (8), b_0 is the distance between O and O_i, as shown in Fig. 1. Moreover,

$$\overrightarrow{OC} = \mathbf{c} = \begin{bmatrix} x \\ y \\ z \end{bmatrix} \tag{10}$$

and

$$\overrightarrow{CP_i} = \frac{p_i}{2\pi}\phi\mathbf{k}, \quad \overrightarrow{CP_1} = \frac{p_1}{2\pi}\phi\mathbf{k}, \quad \overrightarrow{CP_2} = \frac{p_2}{2\pi}\phi\mathbf{k} \tag{11}$$

In the first of Eqs. (11), p_i is the pitch of the ith H pair.

Upon substituting Eqs. (3–11) into Eqs. (1) and (2), one obtains two corresponding expressions for the same vector $\mathbf{p}_i$, namely,

$$\mathbf{p}_i = d_i\mathbf{a}_i + r_i\mathbf{u}_i(\theta_i) + l_i\mathbf{v}_i(\theta_i, \lambda_i) \tag{12}$$

$$\mathbf{p}_i = -b_{0i}\mathbf{k} + \mathbf{c} + \frac{p_i}{2\pi}\phi\mathbf{k} \tag{13}$$

Next if the right-hand sides of Eqs. (1) and (2) are equated, thereby closing the loop, one obtains

$$d_i\mathbf{a}_i + r_i\mathbf{u}_i(\theta_i) + l_i\mathbf{v}_i(\theta_i, \lambda_i) = -b_{0i}\mathbf{k} + \mathbf{c} + \frac{p_i}{2\pi}\phi\mathbf{k} \tag{14}$$

which is the mechanism *loop-closure equation*.

3.2. Inverse Displacement Analysis

For the inverse displacement analysis, the actuator-joint variables, d_1, d_2, θ_1 and θ_2, are to be obtained as functions of the position vector $\mathbf{c} = [x, y, z]^T$ and angle ϕ, which define the pose of the MP.

Upon pre-multiplying the expression $\mathbf{p}_i$ of Eq. (12) by $\mathbf{a}_i^T$, one obtains

$$\mathbf{a}_i^T\mathbf{p}_i = d_i\mathbf{a}_i^T\mathbf{a}_i + r_i\mathbf{a}_i^T\mathbf{u}_i(\theta_i) + l_i\mathbf{a}_i^T\mathbf{v}_i(\theta_i, \lambda_i) = d_i \tag{15}$$

Note that by design, $\mathbf{a}_i$ is perpendicular to both $\mathbf{u}_i$ and $\mathbf{v}_i$, i.e.,

$$\mathbf{a}_i^T\mathbf{u}_i = 0, \quad \mathbf{a}_i^T\mathbf{v}_i = 0 \tag{16}$$

Furthermore, upon pre-multiplying $\mathbf{p}_i$ of Eq. (13) by $\mathbf{a}_i^T$, for $i = 1, 2$, one obtains

$$\begin{aligned}\mathbf{a}_1^T \mathbf{p}_1 &= \mathbf{i}^T (b_0\mathbf{k} + \mathbf{c} + \frac{p_1}{2\pi}\phi\mathbf{k}) \\ &= \begin{bmatrix} 1 & 0 & 0 \end{bmatrix} \left(\begin{bmatrix} 0 \\ 0 \\ b_0 \end{bmatrix} + \begin{bmatrix} x \\ y \\ z \end{bmatrix} + \begin{bmatrix} 0 \\ 0 \\ \frac{p_1}{2\pi}\phi \end{bmatrix} \right) = x \end{aligned} \tag{17}$$

$$\begin{aligned}\mathbf{a}_2^T \mathbf{p}_2 &= \mathbf{j}^T (-b_0\mathbf{k} + \mathbf{c} + \frac{p_2}{2\pi}\phi\mathbf{k}) \\ &= \begin{bmatrix} 0 & 1 & 0 \end{bmatrix} \left(\begin{bmatrix} 0 \\ 0 \\ -b_0 \end{bmatrix} + \begin{bmatrix} x \\ y \\ z \end{bmatrix} + \begin{bmatrix} 0 \\ 0 \\ \frac{p_2}{2\pi}\phi \end{bmatrix} \right) = y \end{aligned} \tag{18}$$

From Eqs. (15–18), d_1 and d_2 are readily obtained as

$$d_1 = x, \quad d_2 = y \tag{19}$$

Equations (19) are apparent that d_i is the projection of vector $\mathbf{p}_i$ on to the x-axis for $i = 1$ and the y-axis for $i = 2$.

Next, to obtain angle θ_i of the ith actuated joint, Eqs. (12–14) are rearranged.

$$\mathbf{p}_i - d_i\mathbf{a}_i = r_i\mathbf{u}_i(\theta_i) + l_i\mathbf{v}_i(\theta_i, \lambda_i) \tag{20}$$

Note here that $\mathbf{p}_i$ and $d_i\mathbf{a}_i$ are known. For simplicity, the left-hand side of Eq. (20) is defined as $\mathbf{q}_i$, Eq (20) then leading to

$$l_i\mathbf{v}_i(\theta_i, \lambda_i) = \mathbf{q}_i - r_i\mathbf{u}_i(\theta_i) \tag{21}$$

In order to eliminate the passive joint variable λ_i, appearing in $\mathbf{v}_i(\theta_i, \lambda_i)$, both sides of Eq. (21) are premultiplied by their corresponding transpose.

$$l_i^2\mathbf{v}_i^T\mathbf{v}_i = \mathbf{q}_i^T\mathbf{q}_i - 2r_i\mathbf{q}_i^T\mathbf{u}_i + r_i^2\mathbf{u}_i^T\mathbf{u}_i$$

or

$$l_i^2 = \mathbf{q}_i^T\mathbf{q}_i' - 2r_i\mathbf{q}_i^T\mathbf{u}_i + r_i^2 \tag{22}$$

Upon rearranging of the foregoing equation,

$$2r_i\mathbf{q}_i^T\mathbf{u}_i = \mathbf{q}_i^T\mathbf{q}_i + r_i^2 - l_i^2 \tag{23}$$

Next, Eq. (5) is substituted into Eq. (23), to obtain

$$2r_i\mathbf{q}_i^T(\cos\theta_i\mathbf{x}_i + \sin\theta_i\mathbf{y}_i) = \mathbf{q}_i^T\mathbf{q}_i + r_i^2 - l_i^2$$

where θ_i is obtained from the relation

$$(\mathbf{q}_i^T\mathbf{y}_i)\sin\theta_i + (\mathbf{q}_i^T\mathbf{x}_i)\cos\theta_i - \frac{\mathbf{q}_i^T\mathbf{q}_i + r_i^2 - l_i^2}{2r_i} = 0 \tag{24}$$

By applying the *tan-half-angle identities* [5], θ_i is solved as

$$\theta_i = 2\arctan\left(\frac{-e_1 \pm \sqrt{e_1^2 + e_2^2} - e_3^2}{e_3 - e_2}\right) \tag{25}$$

with the definitions

$$e_1 = \mathbf{q}_i^T \mathbf{y}_i, \quad e_2 = \mathbf{q}_i^T \mathbf{x}_i, \quad e_3 = -\frac{\mathbf{q}_i^T \mathbf{q}_i + r_i^2 - l_i^2}{2r_i} \tag{26}$$

Furthermore, the unit vector $\mathbf{v}_i$ of the distal link is given from Eq. (21) as

$$\mathbf{v}_i = \frac{\mathbf{q}_i - r_i \mathbf{u}_i}{l_i} \tag{27}$$

3.3. Forward Displacement Analysis

In this case, the position $\mathbf{c} = [x, y, z]^T$ and the orientation ϕ of the MP are determined as functions of the prescribed actuated-joint variables, d_i and θ_i, for $i = 1, 2$. From Eqs. (19), the coordinates x and y of the MP are given *directly* in terms of the actuated-joint variables d_1 and d_2, which need no further work, i.e.,

$$x = d_1, \quad y = d_2 \tag{28}$$

The loop-closure equations (14) are now expressed in vector form as

$$\begin{bmatrix} d_1 \\ 0 \\ 0 \end{bmatrix} + \begin{bmatrix} 0 \\ r_1 \cos\theta_1 \\ r_1 \sin\theta_1 \end{bmatrix} + \begin{bmatrix} 0 \\ l_1 \cos(\theta_1 + \lambda_1) \\ l_1 \sin(\theta_1 + \lambda_1) \end{bmatrix} = \begin{bmatrix} 0 \\ 0 \\ b_0 \end{bmatrix} + \begin{bmatrix} x \\ y \\ z \end{bmatrix} + \begin{bmatrix} 0 \\ 0 \\ \frac{p_1}{2\pi}\phi \end{bmatrix} \tag{29}$$

$$\begin{bmatrix} 0 \\ d_2 \\ 0 \end{bmatrix} + \begin{bmatrix} r_2 \sin\theta_2 \\ 0 \\ r_2 \cos\theta_2 \end{bmatrix} + \begin{bmatrix} l_2 \sin(\theta_2 + \lambda_2) \\ 0 \\ l_2 \cos(\theta_2 + \lambda_2) \end{bmatrix} = \begin{bmatrix} 0 \\ 0 \\ -b_0 \end{bmatrix} + \begin{bmatrix} x \\ y \\ z \end{bmatrix} + \begin{bmatrix} 0 \\ 0 \\ \frac{p_2}{2\pi}\phi \end{bmatrix} \tag{30}$$

From the first row of Eq. (30) and the first of Eqs. (28), one obtains

$$d_1 = r_2 \sin\theta_2 + l_2 \sin(\theta_2 + \lambda_2) \tag{31}$$

Whence, the passive-joint angle λ_2 is derived as

$$\lambda_2 = \arcsin\left(\frac{d_1 - r_2 \sin\theta_2}{l_2}\right) - \theta_2 \tag{32}$$

Likewise, the passive-joint variable λ_1 is derived from the second row of Eq. (29) and the second of Eqs. (28) as

$$d_2 = r_1 \cos\theta_1 + l_1 \cos(\theta_1 + \lambda_1), \quad \lambda_1 = \arccos\left(\frac{d_2 - r_1 \cos\theta_1}{l_1}\right) - \theta_1 \tag{33}$$

Moreover, from the third rows of Eqs. (29) and (30), we have

$$b_0 + z + \frac{p_1}{2\pi}\phi = r_1 \sin\theta_1 + l_1 \sin(\theta_1 + \lambda_1) \tag{34a}$$

$$-b_0 + z + \frac{p_2}{2\pi}\phi = r_2 \cos\theta_2 + l_2 \cos(\theta_2 + \lambda_2) \tag{34b}$$

The right-hand sides of Eqs. (34a & b) are known because λ_1 and λ_2 have already been derived in Eqs. (32) and (33), respectively, while z and ϕ are obtained from the relation below:

$$\begin{bmatrix} 1 & p_1/2\pi \\ 1 & p_2/2\pi \end{bmatrix} \begin{bmatrix} z \\ \phi \end{bmatrix} = \begin{bmatrix} r_1 \sin\theta_1 + l_1 \sin(\theta_1 + \lambda_1) - b_0 \\ r_2 \cos\theta_2 + l_2 \cos(\theta_2 + \lambda_2) + b_0 \end{bmatrix} \tag{35}$$

which can be solved for z and ϕ as long as the coefficient matrix on the left-hand side is non-singular. This is the case as long as $p_1 \neq p_2$, i.e., as long as the pitches of the two H joints of the MP are distinct.

4. JACOBIAN ANALYSIS

4.1. Jacobian Matrices of the Peppermill

The two Jacobian matrices of the Peppermill are derived by applying the approach based on virtual displacements to the loop closure equation (14), as proposed by Arai [6], thereby deriving

$$\begin{aligned}\delta d_i\mathbf{a}_i + d_i\delta\mathbf{a}_i + \delta r_i\mathbf{u}_i(\theta_i) + r_i\delta\mathbf{u}_i(\theta_i) + \delta l_i\mathbf{v}_i + l_i\delta\mathbf{v}_i \\ = -\delta b_{0i}\mathbf{k} - b_{0i}\delta\mathbf{k} + \delta\mathbf{c} + \left(\frac{\delta p_i}{2\pi}\phi + \frac{p_i}{2\pi}\delta\phi\right)\mathbf{k} + \frac{p_i}{2\pi}\phi\,\delta\mathbf{k}\end{aligned} \tag{36}$$

Further it is recalled that the link lengths r_i and l_i, the pitch p_i of the H joint, and the unit vectors $\mathbf{a}_i$ and $\mathbf{k}_i$ are constant. Hence, the variations undergone by these quantities, as appearing in Eq. (36), vanish, Eq. (36) thus simplifying to

$$\delta d_i\mathbf{a}_i + r_i\delta\mathbf{u}_i + l_i\delta\mathbf{v}_i = \delta\mathbf{c} + \frac{p_i}{2\pi}\delta\phi\mathbf{k} \tag{37}$$

From Eq. (5),

$$\delta\mathbf{u}_i = \delta(\cos\theta_i\mathbf{x}_i + \sin\theta_i\mathbf{y}_i) = (-\sin\theta_i\mathbf{x}_i + \cos\theta_i\mathbf{y}_i)\delta\theta = \mathbf{u}_{\theta i}\delta\theta \tag{38}$$

Substituting Eq. (38) into Eq. (37), one obtains

$$\delta d_i\mathbf{a}_i + r_i\mathbf{u}_{\theta i}\delta\theta_i + l_i\delta\mathbf{v}_i = \delta\mathbf{c} + \frac{p_i}{2\pi}\delta\phi\mathbf{k} \tag{39}$$

Upon pre-multiplying both sides of Eq. (39) by $\mathbf{a}_i^T$ and by $\mathbf{v}_i^T$, two additional relations are obtained:

$$\delta d_i\mathbf{a}_i^T\mathbf{a}_i + r_i\mathbf{a}_i^T\mathbf{u}_{\theta i}\delta\theta_i + l_i\mathbf{a}_i^T\delta\mathbf{v}_i = \mathbf{a}_i^T\delta\mathbf{c} + \frac{p_i}{2\pi}\delta\phi\mathbf{a}_i^T\mathbf{k} \tag{40}$$

$$\delta d_i\mathbf{v}_i^T\mathbf{a}_i + r_i\mathbf{v}_i^T\mathbf{u}_{\theta i}\delta\theta_i + l_i\mathbf{v}_i^T\delta\mathbf{v}_i = \mathbf{v}_i^T\delta\mathbf{c} + \frac{p_i}{2\pi}\delta\phi\mathbf{v}_i^T\mathbf{k} \tag{41}$$

As shown in Fig. 1, the various vectors involved in the foregoing equations obey the relations (16) plus $\mathbf{a}_i \perp \mathbf{u}_{\theta i}$, $\mathbf{a}_i \perp \delta\mathbf{v}_i$ and $\mathbf{a}_i \perp \mathbf{k}$. Moreover, since $\mathbf{v}_i$ has a constant magnitude,

$$\mathbf{v}_i^T\delta\mathbf{v}_i = 0 \tag{42}$$

Eqs. (40) and (41) thus reduce to

$$\delta d_i = \mathbf{a}_i^T\delta\mathbf{c}, \quad r_i\mathbf{v}_i^T\mathbf{u}_{\theta i}\delta\theta_i = \mathbf{v}_i^T\delta\mathbf{c} + \frac{p_i}{2\pi}\delta\phi\mathbf{v}_i^T\mathbf{k} \tag{43}$$

with $\delta\mathbf{c}$ representing a small displacement of the position vector of point C of the MP.

Equations (43) express the relationships between the small displacement $\delta\mathbf{c}$ and the small angle $\delta\phi$ of the MP with the small variations of the actuated-joint variables δd_i and $\delta\theta_i$ of the ith driving unit.

The relationship between the small displacements of the MP and those of the actuated joints are expressed below in array form:

$$\begin{bmatrix}\mathbf{a}_1^T & 0\\ \mathbf{a}_2^T & 0\\ \mathbf{v}_1^T & p_1\mathbf{v}_1^T\mathbf{k}/2\pi\\ \mathbf{v}_2^T & p_2\mathbf{v}_2^T\mathbf{k}/2\pi\end{bmatrix}\begin{bmatrix}\delta x\\ \delta y\\ \delta z\\ \delta\phi\end{bmatrix} = \begin{bmatrix}1 & 0 & 0 & 0\\ 0 & 1 & 0 & 0\\ 0 & 0 & \mathbf{v}_1^T\mathbf{u}_{\theta 1} & 0\\ 0 & 0 & 0 & \mathbf{v}_2^T\mathbf{u}_{\theta 2}\end{bmatrix}\begin{bmatrix}\delta d_1\\ \delta d_2\\ r_1\delta\theta_1\\ r_2\delta\theta_2\end{bmatrix} \tag{44}$$

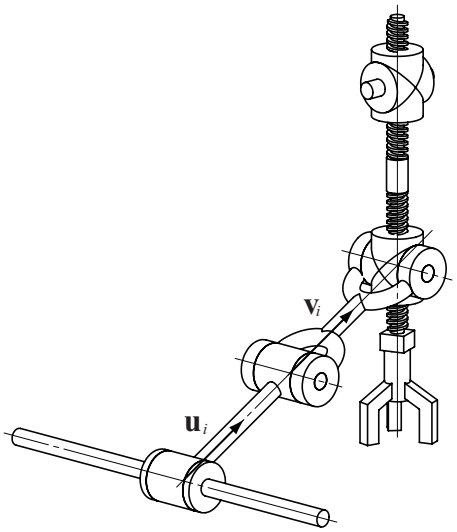

Fig. 2. A robot posture with a singularity of the first kind.

The unit vectors $\mathbf{v}_i$ and $\mathbf{u}_{\theta i}$ are represented componentwise as

$$\mathbf{v}_1 = \begin{bmatrix} 0 \\ v_{1y} \\ v_{1z} \end{bmatrix}, \quad \mathbf{v}_2 = \begin{bmatrix} v_{2x} \\ 0 \\ v_{2z} \end{bmatrix}; \quad \mathbf{u}_{\theta 1} = \begin{bmatrix} 0 \\ u_{\theta 1y} \\ u_{\theta 1z} \end{bmatrix}, \quad \mathbf{u}_{\theta 2} = \begin{bmatrix} u_{\theta 2z} \\ 0 \\ u_{\theta 2z} \end{bmatrix} \tag{45}$$

Upon substitution of the foregoing vectors into Eq. (44), one obtains

$$\mathbf{A}\delta\mathbf{x} = \mathbf{B}\delta\theta \tag{46}$$

where $\mathbf{A}$ and $\mathbf{B}$ are the two Jacobian matrices of the Peppermill, namely,

$$\mathbf{A} = \begin{bmatrix} 1 & 0 & 0 & 0 \\ 0 & 1 & 0 & 0 \\ 0 & v_{1y} & v_{1z} & p_1 v_{1z}/2\pi \\ v_{2x} & 0 & v_{2z} & p_2 v_{2z}/2\pi \end{bmatrix}, \quad \mathbf{B} = \begin{bmatrix} 1 & 0 & 0 & 0 \\ 0 & 1 & 0 & 0 \\ 0 & 0 & \mathbf{v}_1^T\mathbf{u}_{\theta 1} & 0 \\ 0 & 0 & 0 & \mathbf{v}_2^T\mathbf{u}_{\theta 2} \end{bmatrix} \tag{47}$$

4.2. The Singularity of the First Kind

The singularity of the first kind [7], which is also referred to as the inverse-kinematics singularity [8], occurs when the Jacobian matrix $\mathbf{B}$ in the second of Eqs. (47) is singular, i.e., when any of two bottom diagonal entries vanishes.

Geometrically, this singularity occurs when $\mathbf{v}_1 \perp \mathbf{u}_{\theta 1}$ or $\mathbf{v}_2 \perp \mathbf{u}_{\theta 2}$. According to the definition of $\mathbf{u}_{\theta i}$ in Eq. (38), this happens when the unit vector $\mathbf{v}_i$ of the proximal link and the unit vector $\mathbf{u}_i$ of the distal link are parallel in at least one driving unit. Figure 2 illustrates a posture with this kind of singularity.

4.3. The Singularity of the Second Kind

The singularity of the second kind [7], which is also referred to as the direct-kinematics singularity, occurs when the Jacobian matrix $\mathbf{A}$ in the first of Eqs. (47) becomes singular. This singularity is readily established

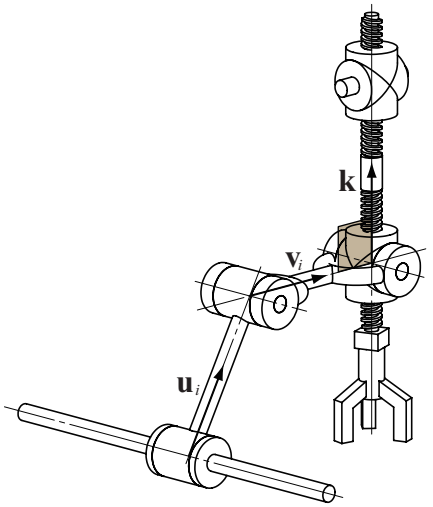

Fig. 3. A robot posture with a singularity of the second kind.

by virtue of the block structure of the matrix, namely,

$$\begin{aligned}
\det(\mathbf{A}) &= \det\left(\left[\begin{array}{cc|cc} 1 & 0 & 0 & 0 \\ 0 & 1 & 0 & 0 \\ \hline 0 & v_{1y} & v_{1z} & p_1 v_{1z}/2\pi \\ v_{2x} & 0 & v_{2z} & p_2 v_{2z}/2\pi \end{array}\right]\right) \\
&= \det\left(\left[\begin{array}{cc} 1 & 0 \\ 0 & 1 \end{array}\right]\right) \det\left(\left[\begin{array}{cc} v_{1z} & p_1 v_{1z}/2\pi \\ v_{2z} & p_2 v_{2z}/2\pi \end{array}\right]\right) \\
&= v_{1z} v_{2z} \frac{p_2 - p_1}{2\pi} = 0
\end{aligned} \tag{48}$$

Therefore, matrix **A** becomes singular whenever one of its three factors vanishes. Geometrically, these conditions occur when

1. The unit vector of the distal link of at least one limb lies in the *xy* plane, i.e., when the unit vector of the distal link of at least one limb is normal to the *z*-axis, and

2. The pitch of the upper H pair equals that of its lower counterpart. This singularity is of the architecture type [9].

Condition 2 can be readily avoided by choosing the pitches of the H pairs distinct. Even better, we chose the pitches of identical absolute values but of opposite signs, i.e., we chose these two pitches identical, but of opposite hands. Figure 3 illustrates a posture with the singularity of the second kind.

4.4. The Singularity of the Third Kind

The singularity of the third kind [7], which is also referred to as the complex-kinematics singularity, occurs when the the two Jacobian matrices **A** and **B** become singular. This singularity is of a different kind, as not every robot admits it. Indeed, this singularity depends on the robot architecture. Given the symmetries with which the Peppermill was designed, this robot admits the singularity of the third kind, as illustrated in Fig. 4.

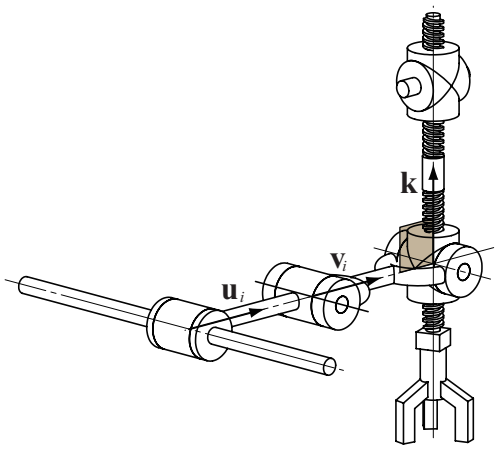

Fig. 4. A robot posture with a singularity of the third kind.

5. CONCLUSIONS

The position and Jacobian analyses of a CRRHHRRC Schönflies motion generator (SMG), dubbed here the Peppermill, were discussed. Vector-loop analysis is applied to derive the position relations of the mechanism. Inverse- and direct-kinematics relations were derived. The two Jacobian matrices were also derived by means of the vector loop equations as applied to virtual displacements. The postures at which the Peppermill finds itself at each of the singularities of the three kinds were identified and illustrated with figures.

ACKNOWLEDGEMENTS

The technical support provided by Damien Trézières, a research trainee from ICAM, in Toulouse, France, is dutifully acknowledged. The first author would like to acknowledge the financial support received from MEXT-supported program for the strategic Research Foundation to Private Universities, 2012–2014. The second author would like to acknowledge the financial support received from NSERC through a Discovery Grant and from McGill University via a James McGill Professorship.

REFERENCES

1. Gauthier, J.F., Angeles, J., Nokleby, S.B. and Morozov, A., "The kinetostatic conditioning of two-limb schönflies motion generators", *Transantions ASME, Journal of Mechanisms and Robotics*, Vol. 1, pp. 011010–1–12, 2009.
2. Pierrot, F. and Company, O., "H4: A new family of 4-dof parallel robots", in *Proceedings of the IEEE/ASME International Conference on Advanced Intelligent Mechatronics*, Atlanta, USA, September 19–23, pp. 508–513, 1999.
3. Company, O., Pierrot, F., Krut, S. and Nabat, V., "Simplified dynamic modelling and improvement of a four-degree-of-freedom pick-and-place manipulator with articulated moving platform", *Proceedings of the Institution of Mechanical Engineers, Part I: Journal of Systems and Control Engineering*, Vol. 223, No. 1, pp. 13–29, 2009.
4. Lee, C.C. and Lee, P.C., "Isoconstraned mechanisms for fast pick-and-place manipulation", in *Geometric Methods in Robotics and Mechanism Research*, Y. Lou and Z. Li (Eds.), LAP Lambert Academic Publishing, pp. 85–99, 2011.
5. Angeles, J., *Fundamentals of Robotic Mechanical Systems: Theory, Methods, and Algorithms*, 3rd ed. Springer, 2007.
6. Arai, T., "Analysis and sythesis of a parallel link manipulator based on its statics", *Journal of the Robotic Society of Japan*, Vol. 10, No. 4, pp. 526–533, 1992 [in Japanese].
7. Gosselin, C. and Angeles, J., "Singulaity analysis of closed-loop kinematic chains", *IEEE Transactions on Robotics and Automation*, Vol. 8, No. 3, pp. 281–290, 1990.

8. Tsai, L.W., *Robot Analysis: The Mechanics of Serial and Parallel Manipulators*. Wiley-Interscience, 1998.
9. Ma, O. and Angeles, J., "Architecture singularities of parallel manipulators", *The International Journal of Robotics and Automation*, Vol. 7, No. 1, pp. 23–29, 1992.

APPENDIX

Appendix A: Conceptual Design of the Cylindrical Joints

Figure A.1 illustrates the conceptual design of the cylindrical joint which is driven by identical rotational motors in a differential array of helical-screw drives.

The relationships between displacement of the cylindrical joint, d_i and θ_i, and the angular displacements of the motors, η_{iL} and η_{iR}, are given below:

$$\frac{p_{iL}}{2\pi}(\eta_{iL}-\theta_i)=d_i, \quad \frac{p_{iR}}{2\pi}(\eta_{iR}-\theta_i)=d_i \tag{A.1}$$

where $p_{iL}>0$ and $p_{iR}<0$ represent the pitches of the left-hand screw and the right-hand screw, respectively. For simplicity, $i(=1,2)$, which represents the number of the cylindrical joint, will be dropped henceforth. In order to simplify the mechanical design and control system of the cylindrical joints, we applied a symmetrical design. The pitches of the screws are expressed by means of common pitch $p_c(>0)$ as,

$$p_L=p_c, \quad p_R=-p_c \tag{A.2}$$

From Eqs. (A.1–A.2), relationships between the displacement of the cylindrical joint, d and θ, and angular displacements of the motors, η_L and η_R, in the symmetrical design are expressed by a system of two linear equations, namely,

$$\frac{p_c}{2\pi}\begin{bmatrix}1 & 0\\ 0 & -1\end{bmatrix}\begin{bmatrix}\eta_L\\ \eta_R\end{bmatrix}=\begin{bmatrix}1 & p_c/2\pi\\ 1 & -p_c/2\pi\end{bmatrix}\begin{bmatrix}d\\ \theta\end{bmatrix} \tag{A.3}$$

The inverse displacement relations which give motor variables η_L and η_R in terms of the cylindrical joint valuables d and θ are

$$\begin{bmatrix}\eta_L\\ \eta_R\end{bmatrix}=\frac{2\pi}{p_c}\begin{bmatrix}1 & 0\\ 0 & -1\end{bmatrix}\begin{bmatrix}1 & p_c/2\pi\\ 1 & -p_c/2\pi\end{bmatrix}\begin{bmatrix}d\\ \theta\end{bmatrix}=\begin{bmatrix}2\pi/p_c & 1\\ -2\pi/p_c & 1\end{bmatrix}\begin{bmatrix}d\\ \theta\end{bmatrix} \tag{A.4}$$

Likewise, the forward displacement relations are

$$\begin{bmatrix}d\\ \theta\end{bmatrix}=\frac{p_c}{2\pi}\begin{bmatrix}1 & p_c/2\pi\\ 1 & -p_c/2\pi\end{bmatrix}^{-1}\begin{bmatrix}1 & 0\\ 0 & -1\end{bmatrix}\begin{bmatrix}\eta_L\\ \eta_R\end{bmatrix}=\begin{bmatrix}p_c/2\pi & -p_c/2\pi\\ 1/2 & 1/2\end{bmatrix}\begin{bmatrix}\eta_L\\ \eta_R\end{bmatrix} \tag{A.5}$$

Since the two foregoing relations are linear, the actuator Jacobian $\mathbf{J}_c$, that maps motor angular velocities into actuator rates, is identical the matrix coefficient in the rightmost-hand side of Eq. (A.5).

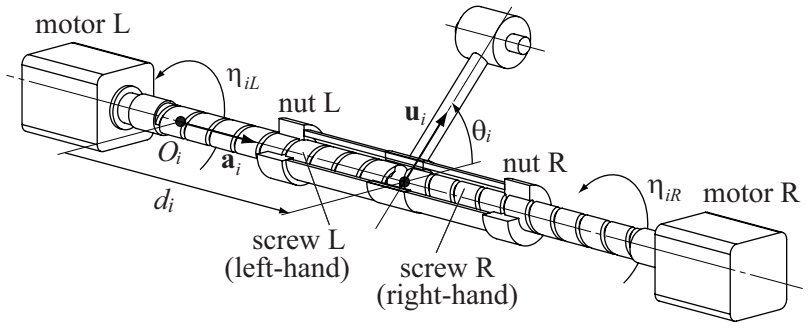

Fig. A.1. Conceptual design of the cylindrical joint.